NUCLEAR THEORY, Vol. 32 (2013)
eds. A.I. Georgieva, N. Minkov, Heron Press, Sofia

Calculations of the Pion-Nucleus Inelastic Cross Sections Using the Microscopic Optical Potential

K.V. Lukyanov[1], **V.K. Lukyanov**[1], **E.V. Zemlyanaya**[1], **A.Y. Ellithi**[2], **I.A.M. Abdel-Magead**[2]

[1]Joint Institute for Nuclear Research, 141980 Dubna, Russia
[2]Cairo University, Cairo, Giza, Egypt

Abstract. The calculations of the pion-nucleus inelastic scattering are made using the microscopic optical potential (OP), developed basing on the elementary pion-nucleon scattering amplitude and the density distribution function of a target nucleus. Within this OP the elastic scattering data on Si, Ni and Pb were explained by solving the relativistic wave equation, and then the same parameters are applied for estimations of the respective data on inelastic cross sections. In calculations, the microscopic transition potential was constructed with a help of a derivative of the density distribution functions of a target nucleus. The results obtained for inelastic cross sections are discussed and compared to the existing experimental data.

1 Statement of the Problem

In the preceding paper [1], the microscopic optical potential (OP) $U_{el}(r)$ [2] was utilized for calculations of elastic scattering differential cross sections and thus there were successfully explained the data on the $\pi^{\pm}$-meson scattering on nuclei ^{28}Si, ^{58}Ni, ^{208}Pb at $T_{\rm lab} = 291$ MeV [3]. In fact this OP is a folding integral of the nuclear density distribution function and the elementary pion-nucleon amplitude of scattering. The parameters of the latter $\pi^{\pm}N$-amplitude were fitted and their in-medium magnitudes were established and compared with those for pions scattered on free nucleons (see below in Table 1).

In the present work we are basing on the obtained potentials to derive the transition optical potentials (TOP) $U_{inel}(\mathbf{r}, \xi)$ depended on the collective variables of nuclei. These TOPs provide calculations of the pion-nucleus inelastic scattering with excitations of the quadruple 2^+ and octuple 3^- collective states of the same nuclei. This scheme does not contain free parameters except the static or dynamic deformation parameters β_λ, that characterize the structure of their rotational or vibration excited states of nuclei. As to a transition potential, it can be constructed in two forms, one corresponds to a derivative of the microscopic OP with respect to the deformation admixture to the relative motion radius-vector, and the other one uses the derivative of the target nucleus

density distribution under the folding integral of a microscopic OP. So if one gets the elastic and transition potentials, then the respective inelastic scattering cross sections can be calculated utilizing the DWUCK4 program [4]. To this end one should preliminary transform the relativistic wave equation inherent in a πA scattering to the standard non-relativistic form. Doing so the relativistic and distortions effects in initial and final channels are accounted for automatically.

2 The Model and Methodical Estimations

We start with the microscopic OP developed in [2] and given in the following form:

$$U_{\rm opt}(r) = -\frac{(\hbar c)\beta_c}{2(2\pi)^3}\sigma[i+\alpha]\cdot\int {\rm e}^{-i\mathbf{qr}}\rho(\mathbf{q})f(q)q^2dq. \qquad (1)$$

Here $\rho(q)$ is the form factor of a spherically-symmetric density distribution function of bare nucleons in a nucleus normalized to mass number A

$$\rho(\mathbf{q}) = \int {\rm e}^{i\mathbf{qr}}\rho(\mathbf{r})d^3r. \qquad (2)$$

In our calculations [1] of elastic scattering of pions on nuclei, the densities $\rho(r)$ were taken to be in the form of fermi functions with parameters R and a (in fm) equal to 3.134 and 0.477 for ^{28}Si [5]; 4.2 and 0.475 for ^{58}Ni [6]; 6.654 and 0.475 for ^{208}Pb [7]. The other values in (1), σ and α are the averaged over isospins total πN cross sections and the ratio of real to imaginary part of the pion-nucleon amplitude at forward angles of scattering. The amplitude itself has the form

$$F_{\pi N}(q) = \frac{k}{4\pi}\sigma[i+\alpha]\cdot f(q), \qquad f(q) = {\rm e}^{-\beta_\pi q^2/2}. \qquad (3)$$

where β_π is the slope parameter. For scattering of pions on free protons $\beta_\pi = 0.434$ fm^2, and the averaged parameters σ and α are done in refs. [8] and [9] at energies $T_{\rm lab}$ from 90 to 280 MeV. Their magnitudes at 291 MeV were established in [1] basing on the best fit analysis of the elastic scattering data [3] and are presented in Table 1. Starting from these values for free amplitudes, the respective "in-medium" best-fit parameters σ and α were obtained in [1] too by adjusting the calculated pion-nucleus differential cross sections to the experimental data [3] leaving the parameter $\beta_\pi = 0.434$ fm^2 to be the same as for scattering on free protons.

In this way the obtained microscopic OP (1) was then inserted into the Klein-Gordon-Fock relativistic wave equation, where the terms $(U/E)^2 \ll 1$ were neglected and thus it was transformed to the non-relativistic form

$$(\Delta + k^2)\psi(\mathbf{r}) = 2\bar{\mu}\cdot[U_{\rm opt}(r) + U_c(r)]\,\psi(\mathbf{r}), \qquad (4)$$

where the relativistic velocity $\beta_c = v_{\rm c.m.}/c = k_{\rm lab}/[E_{\rm lab} + m_\pi^2/M_A]$ is expressed through the energy $E_{\rm lab} = (k_{\rm lab}^2 + m_\pi^2)^{1/2} = T_{\rm lab} + m_\pi$ and mo-

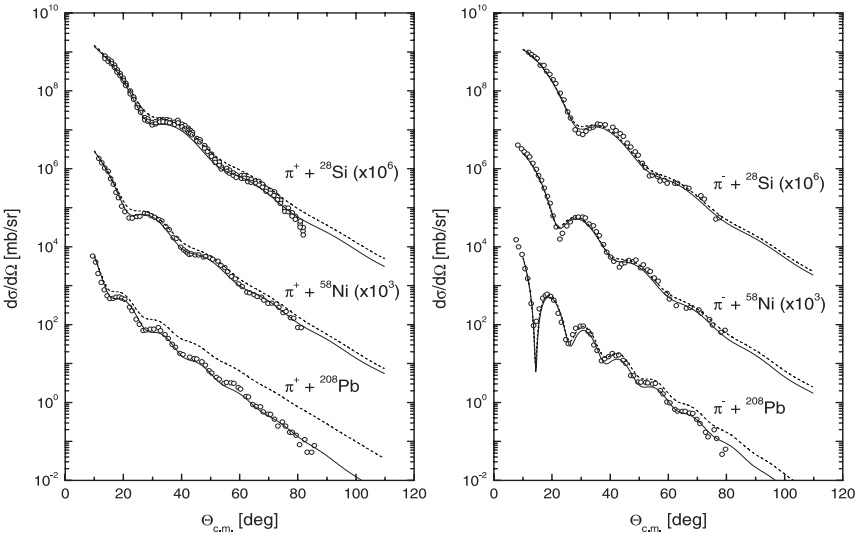

Figure 1. Comparisons of calculated differential cross sections of $\pi^{\pm}$-mesons scattered on nuclei ^{28}Si, ^{58}Ni, ^{208}Pb at $T_{\rm lab} = 291$ MeV to experimental data when using the parameters obtained in [1] (see Table 1). Dashed curves are for parameters of free πN amplitudes, solid lines are for the fitted parameters.

mentum $k_{\rm lab}$[1] with M_A, the mass of a target nucleus. Here the Coulomb potential is taken for the charged sphere with the radius $R_c = r_c A^{1/3}$, where $r_c = 1.3$ fm. Also, k is the relativistic momentum in center of mass system $k = M_A\sqrt{T_{\rm lab}(T_{\rm lab}+2m_\pi)}/\sqrt{(m_\pi+M_A)^2+2M_AT_{\rm lab}}$ and the relativistic reduce mass $\bar{\mu} = \bar{m}_\pi M_A/(\bar{m}_\pi + M_A)$ with $\bar{m}_\pi = \sqrt{k^2+m_\pi^2} = E_{\rm c.m.}$. Finally, the transformed wave equation (4) was computed using the programm DWUCK4 [4], and thus this approach automatically accounts for effects of relativization and also distortions of the relative motion wave functions in the field of a target nucleus. As a result, the elastic scattering differential cross sections were obtained in [1] as shown in Figure 1 by dashed and solid curves in relation to the free and in-medium (fitted) parameters of the πN scattering amplitude.

Now, once parameters of the microscopic OP (1) have been established from the data on the pion-nucleus elastic scattering, we can construct the respective transition potentials for calculations of inelastic scattering of pions with excitation of the low lying 2^+ and 3^- collective states in the same nuclei at the same incident energy. To this end one can use the standard prescription when one deforms the equidensity surfaces of an elastic scattering OP. However it is more naturally to deform the surfaces of a target nucleus densities $\rho(\mathbf{r})$ in (1, 2) by

[1] In Eq. (1), it is useful to use units MeV and fm, and then $\hbar c = 197.327$ MeV·fm. In the other cases we use the natural system of units where $\hbar = c = 1$, and thus E, T, k, m have the same dimension [MeV].

exchanging the r by $\mathbf{r}$ as follows [10]

$$\boldsymbol{r} \Rightarrow r + \delta^{(\lambda)}(\boldsymbol{r}), \quad \delta^{(\lambda)}(\boldsymbol{r}) = -r(r/R)^{\lambda-2} \sum_{\mu} \alpha_{\lambda\mu} Y_{\lambda\mu}(\hat{r}), \quad \lambda = 2, 3, \quad (5)$$

where $\alpha_{\lambda\mu}$ are variables of the collective motion of a nucleus (the angles of rotations or dynamic deviations relative the static "r").

Substituting (5) in the density (2) and then in the potential (1), and terminating their expansions at linear terms in $\delta^{(\lambda)}(\mathbf{r})$ one obtains densities

$$\rho(\mathbf{r}) = \rho(r) + \rho_\lambda(r) \sum_{\mu} \alpha_{\lambda\mu} Y_{\lambda\mu}(\hat{r}), \quad \rho_\lambda(r) = -r \frac{d\rho(r)}{dr} (r/R)^{\lambda-2}, \quad (6)$$

and then their form factors

$$\rho(\mathbf{q}) = \rho(q) + \rho_\lambda(q) i^\lambda \sum_{\mu} \alpha_{\lambda\mu} Y_{\lambda\mu}(\hat{q}), \quad (7)$$

where

$$\rho(q) = 4\pi \int j_0(qr)\rho(r) r^2 dr, \quad \rho_\lambda(q) = 4\pi \int j_\lambda(qr)\rho_\lambda(r) r^2 dr. \quad (8)$$

Finally, substituting (8) in (1) one can obtain the respective potentials for elastic and inelastic scattering

$$U(\mathbf{r}) = U_{\text{opt}}(r) + U^{(\lambda)}(\mathbf{r}), \quad U^{(\lambda)}(\mathbf{r}) = U_\lambda(r) \sum_{\mu} \alpha_{\lambda\mu} Y_{\lambda\mu}(\hat{r}), \quad (9)$$

where

$$U_{\text{opt}}(r) = -\frac{\hbar v}{(2\pi)^2} \sigma\,(i + \alpha) \int j_0(qr)\rho(q) f(q)\, q^2 dq, \quad (10)$$

$$U_\lambda(r) = -\frac{\hbar v}{(2\pi)^2} \sigma\,(i + \alpha) \int j_\lambda(qr)\rho_\lambda(q) f(q) q^2 dq. \quad (11)$$

Here the spherically symmetric part $U_{\text{opt}}(r)$ provides elastic scattering calculations while the $U_\lambda(r)$ is the transition OP used for calculations of inelastic scattering cross sections with excitations of the 2^+ and 3^- collective states of nuclei. In this process the Coulomb interaction is also entered consisting of two parts $U^{(c)}(r)$ and $U^{(c)}_\lambda$, that correspond to the deformed unified charge density sphere of the radius $R = R_c[1 + \sum_\mu \alpha_{\lambda\mu} Y_{\lambda\mu}(\hat{R})]$, $R_c = r_{oc} A^{1/3}$. The amplitude of inelastic scattering is constructed in the framework of the distorted wave Born approximation (DWBA) where the respective matrix element has a linear dependence on the transition $\bar{U}_\lambda = U_\lambda(r) + U^{(c)}_\lambda(r)$ and the distorted waves in initial and final channels $\chi^{(\pm)}(\mathbf{r})$ are calculated using the $U_{\text{opt}}(r) + U^{(c)}(r)$ potential, and thus

$$T_{BA} = \sum_{\mu} \langle B|\alpha_{\lambda\mu}|A\rangle \int \chi^{(-)*}(\mathbf{r}_b)[\bar{U}_\lambda(r) Y_{\lambda\mu}(\hat{r})]\chi^{(+)}(\mathbf{r}_a) d\mathbf{r}_a d\mathbf{r}_b. \quad (12)$$

Here the structure matrix element $\langle B|\alpha_{\lambda\mu}|A\rangle$ provides transition from the ground to excited state of a nucleus. In the case of even-even nuclei one has $|A\rangle = |I_A, M_A\rangle$ ($I_A = M_A = 0$), $\langle B| = \langle I_B, M_B|$ ($I_A = \lambda, M_A = \mu$), and the transition matrix element is [10]

$$\langle B|\alpha_{\lambda\mu}|A\rangle = (I_A\,\lambda M_A\mu|I_B M_B)\langle I_B||\alpha_{\lambda 0}||I_A\rangle$$
$$= (0\,\lambda\,0\,\mu|\lambda\,\mu)\langle\lambda||\alpha_{\lambda 0}||0\rangle = (1/\sqrt{2\lambda+1})\beta_\lambda \quad (13)$$

where β_λ (λ = 2,3) is a deformation parameter which is fitted in our study.

Numerical calculations of the amplitude (12) are made using the DWUCK4 program [4] where input data include the optical potential (10) for computing distorted waves $\chi^{\pm}$, and the transition potential (11) to get differential cross sections. As to the Coulomb transition potential, it has yet incorporated in the DWUCK4 program in the form that corresponds to the external part of a unified charge distribution

$$U_\lambda^{(c)}(r) \;=\; \frac{3Z_A Z_\pi e^2}{2\lambda+1}\cdot\frac{R_c^\lambda}{r^{\lambda+1}}, \qquad r > R_c \quad (14)$$

Below we will consider and analyze results of our calculations of inelastic scattering of $\pi^{\pm}$-mesons on the even-even nuclei ^{28}Si, ^{58}Ni, ^{208}Pb at $T_{\rm lab} = 291$ MeV with excitations of the low-lying 2^+ and 3^- collective states. At first, in Figure 2 we show some results useful for the further applications when analyzing experimental data. So, Figure 2(a) exhibits as an example the nuclear potentials calculated for π^+ scattering from the nucleus ^{208}Pb. It is seen that both the real part of OP, its spherical symmetric part $U_{\rm opt}(r)$ and the transition one $U_{\lambda=3}(r)$, are positive, while the corresponding imaginary parts are negative. Then the overall contributions of $U_{\rm opt}$ to elastic scattering and $U_{\lambda=3}$ to inelastic one are seen to be of comparable values. This allows to assume that the respective inelastic cross section will be smaller the elastic one in about a factor β_λ^2. Then, Figure 2(b) exhibits effect of the Coulomb transition potential on inelastic scattering cross sections. The solid curve shows excitations by both the nuclear and Coulomb transition potentials $U_\lambda + U_\lambda^{(c)}$ while the dot curve demonstrate the case of the nuclear contribution only. One sees that the admixture of the Coulomb excitation provides a weak destructive interference at small angles and practically does not affect cross sections at larger angles. This effect at high energy collision is responsible to that Coulomb interaction, estimated e.g. for the ^{208}Pb to be $U_c(R_c) \simeq 16$ MeV, and for the $U_3^{(c)}(R_c) \simeq (3Ze^2/7R) \simeq 8$ MeV that occur very small as compared to the corresponding values for the hitherto estimated nuclear potentials. The other methodical Figure 2(c) shows calculations of inelastic cross sections with excitation of the 3^- state when we utilized parameters of the free π^+N-amplitude (dotted curve) and of the "in-medium" one (solid curve) (see them in Table 1 below). One can see how it is important to account for the in-medium effect when calculating inelastic scattering. One

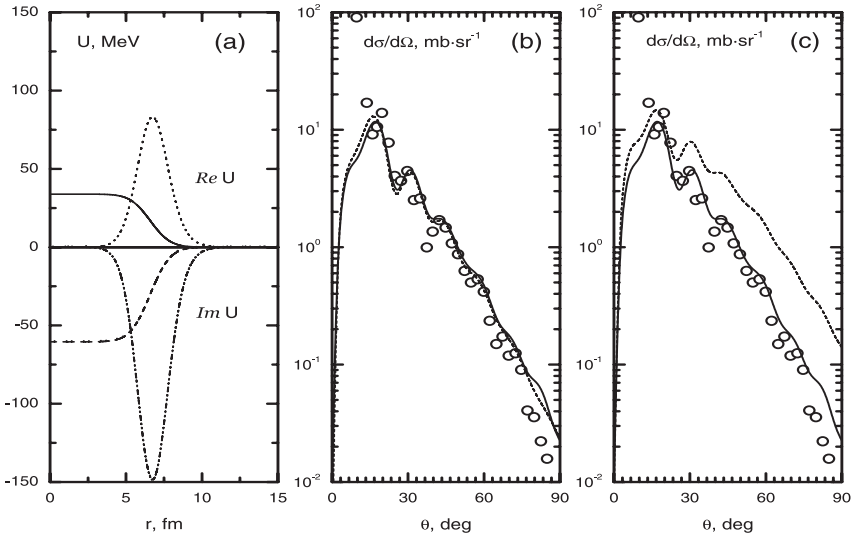

Figure 2. Methodical calculations for ^{208}Pb: (a) nuclear potentials, where solid and dash curves are for $U_{\rm opt}$, dots and dash-dots are for U_λ, real and imaginary parts respectively; (b) effect of the Coulomb excitation on inelastic cross sections, where solid curve - for both the nuclear and Coulomb transition potentials, dots are for the nuclear transition OP only; (c) in-medium effect, where solid curve - for in-medium parameters, dots are for free one.

should note that as is seen from Figure 1 this effect is also significant to elastic scattering cross sections of $\pi^+ + ^{208}$Pb, while for another target nuclei such a discrepancy is not too large, and thus for them the in-medium effect on inelastic scattering will not be so appreciable.

3 Comparisons with Experimental Data

The proposed scheme is distinguished from usually used models by that it operates with the main characteristic of a target nucleus, the density distribution function, while the other models are based from the beginning on an optical potential of elastic scattering. Thus when utilizing the microscopic elastic and transition OPs (9)-(11) we fit the only structure parameter, the deformation (static or dynamic) of a target nucleus. In calculations of inelastic scattering cross sections of $\pi^\pm$-meson of nuclei ^{28}Si, ^{58}Ni, ^{208}Pb $T_{\rm lab} = 291$ MeV we used the in-medium parameters [1] of the $\pi^\pm N$ amplitude of scattering (3), namely, the total cross section σ and the ratio α of the imaginary to real part of the forward scattering $\pi^\pm N$ amplitude, while the shape parameter β_π is left to be as for the free scattering 0.434 fm^2 (see Table 1). The only fitted parameters were the deformation β_2 for quadruple and β_3 for octuple excitations of 2^+ and 3^- states of nuclei.

Table 1. Parameters σ and α of the in-medium πN amplitudes of scattering obtained in [1] from πA elastic scattering data [3] and the deformation parameters β_λ responsible to the inelastic scattering.

	^{28}Si		^{58}Ni		^{208}Pb		πN
	π^+	π^-	π^+	π^-	π^+	π^-	free
σ, fm^2	5.55	4.81	5.43	4.09	4.04	4.23	4.76
α	-0.64	-0.88	-0.68	-1.02	-0.56	-0.92	-0.95
β_π, fm^2				0.434			
β_2	0.48	0.4	0.19	0.19			
β_3	0.3	0.3	0.15	0.17	0.14	0.13	

Comparisons with the experimental data on the respective inelastic cross sections from [3] are shown in Figures 3–5. It is seen that as a whole our calculations are in a good agreement to experimental data. The deformation parameters were obtained by adjusting the absolute values of cross sections to the data while the forms of theoretical curves are not distorted in this procedure. The obtained deformation parameters are presented in the bottom of Table 1. In general they occur in coincidence in about 10% for scattering of π^+- and π^--mesons on the same nuclei. An exception ($\delta\beta_2 \sim 20\%$) is seen only for the case of scattering on the ^{28}Si nucleus.

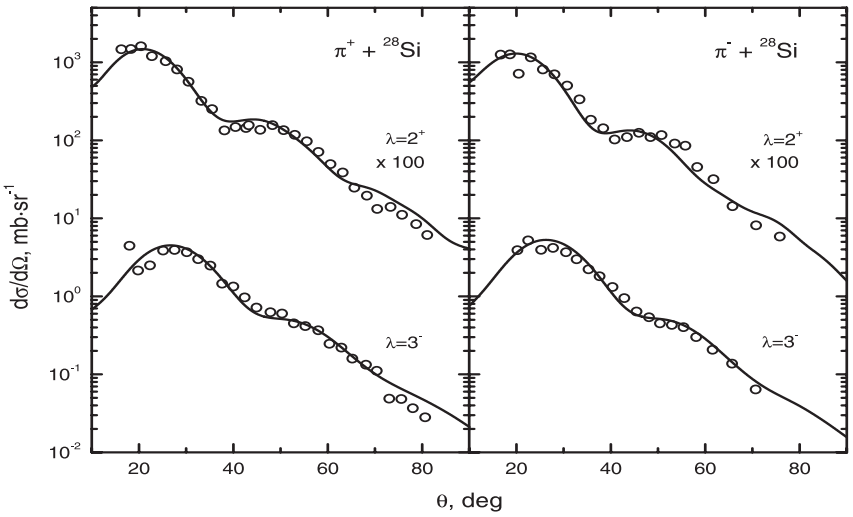

Figure 3. Comparisons of the calculated inelastic scattering cross sections of π-mesons on ^{28}Si at $T_{\rm lab} = 291$ Mev with experimental data from [3] (parameters are from Table 1).

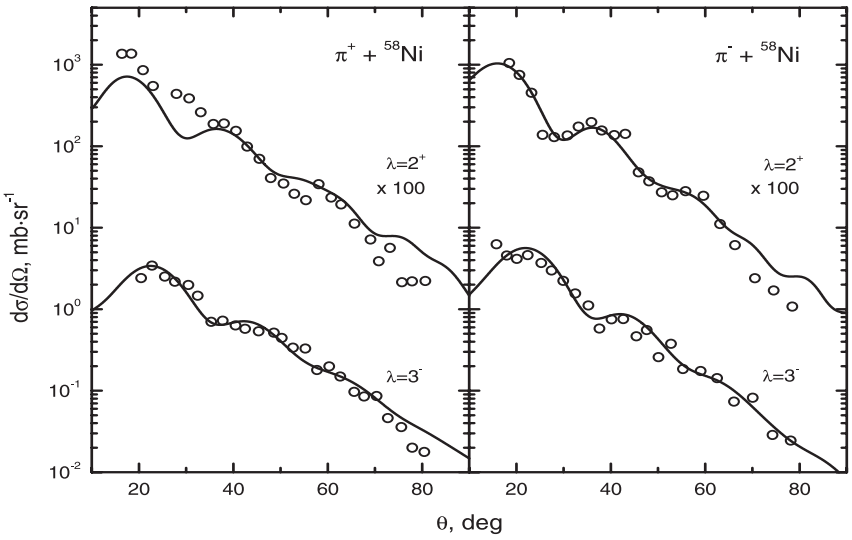

Figure 4. The same as in Figure 3 but for the ^{58}Ni.

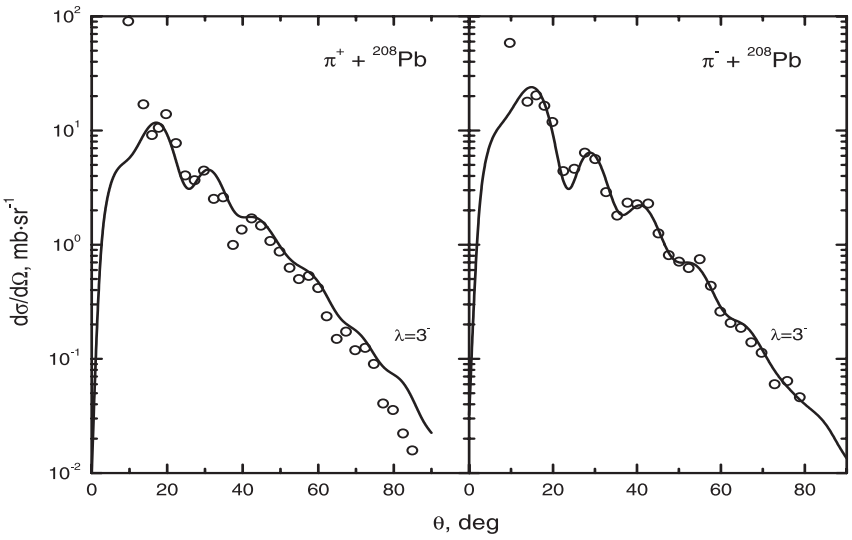

Figure 5. The same as in Figure 3 but for the ^{208}Pb.

Acknowledgements

K.V.L. and E.V.Z. thank the Russian Foundation for Basic Research (Grant Nos. 12-01-00396 and 13-01-00060) for partial support.

References

[1] V.K. Lukyanov, E.V. Zemlyanaya, K.V. Lukyanov *et al.*, *Bull. Russ. Acad. Sci., Physics* **77** (2013) 427.

[2] V.K. Lukyanov, E.V. Zemlyanaya, K.V. Lukyanov, *Phys. Atom. Nucl.* **69** (2006) 240.

[3] D.F. Geesaman, *et al.*, *Phys. Rev. C* **23** (1981) 2635.

[4] P.D. Kunz, E. Rost, in *Computational Nuclear Physics* vol. 2, K. Langanke, *et al.*, Eds. (New York: Springe Verlag, 1993) p. 88.

[5] V.K. Lukyanov, E.V. Zemlyanaya, B. Słowiǹski, *Phys. Atom. Nucl.* **67** (2004) 1282.

[6] M. El-Azab, G.R. Satchler, *Nucl. Phys. A* **438** (2004) 525.

[7] J.D. Patterson, R.J. Peterson, *Nucl. Phys. A.* **77** (2003) 235.

[8] M.P. Locher, O. Steinmann, N. Straumann, *Nucl. Phys. B* **27** (1971) 598.

[9] N. Bano, I. Ahmad, *J. Phys. G* **5** (1979) 39.

[10] R.G. Satchler, *Direct Nuclear Reactions* (Clarendon Press, Oxford, New York, 1983).